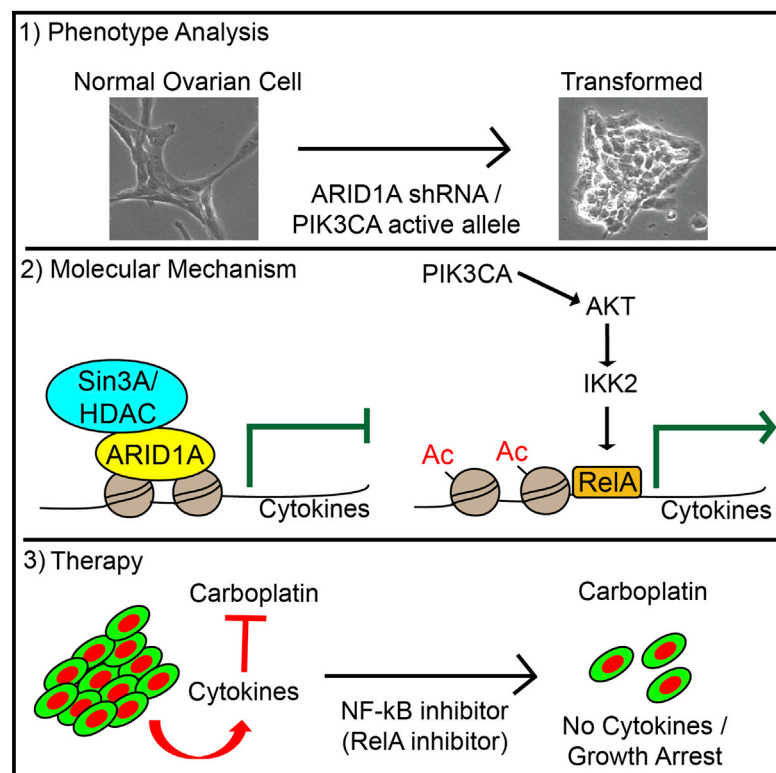Article

Loss of HDAC-Mediated Repression and Gain of NF-κB Activation Underlie Cytokine Induction in ARID1A- and PIK3CA-Mutation-Driven Ovarian Cancer

Graphical Abstract

Authors

Minchul Kim, Falong Lu, Yi Zhang

Correspondence

yzhang@genetics.med.harvard.edu

In Brief

Kim et al. examine the molecular mechanism by which a combination of mutations in a chromatin-modifying factor and a signaling protein contribute to ovarian cancer development.

Highlights

- RelA drives pro-inflammatory cytokine expression in ARID1A/PIK3CA mutant cancers

- PIK3CA releases RelA from IκB through the AKT-IKK2 pathway

- ARID1A recruits Sin3A-HDAC repressor complex to inhibit cytokine gene expression

- An NF-κB inhibitor improves carboplatin efficacy to OCCC with ARID1A/PIK3CA mutations

Accession Numbers

GSE86004

CrossMark

CellPress

Loss of HDAC-Mediated Repression and Gain of NF-κB Activation Underlie Cytokine Induction in ARID1A- and PIK3CA-Mutation-Driven Ovarian Cancer

Minchul Kim,[1,2,3] Falong Lu,[1,2,3] and Yi Zhang[1,2,3,4,5,6,*]
[1]Howard Hughes Medical Institute, Boston Children's Hospital, Boston, MA 02115, USA
[2]Program in Cellular and Molecular Medicine, Boston Children's Hospital, Boston, MA 02115, USA
[3]Division of Hematology/Oncology, Department of Pediatrics, Boston Children's Hospital, Boston, MA 02115, USA
[4]Department of Genetics, Harvard Medical School, Boston, MA 02115, USA
[5]Harvard Stem Cell Institute, WAB-149G, 200 Longwood Avenue, Boston, MA 02115, USA
[6]Lead Contact
*Correspondence: yzhang@genetics.med.harvard.edu
http://dx.doi.org/10.1016/j.celrep.2016.09.003

SUMMARY

ARID1A is frequently mutated in ovarian clear cell carcinoma (OCCC) and often co-exists with activating mutations of PIK3CA. Although induction of pro-inflammatory cytokines has been observed in this cancer, the mechanism by which the two mutations synergistically activate cytokine genes remains elusive. Here, we established an in vitro model of OCCC by introducing ARID1A knockdown and mutant PIK3CA into a normal human ovarian epithelial cell line, resulting in cell transformation and cytokine gene induction. We demonstrate that loss of ARID1A impairs the recruitment of the Sin3A-HDAC complex, while the PIK3CA mutation releases RelA from IκB, leading to cytokine gene activation. We show that an NF-κB inhibitor partly attenuates the proliferation of OCCC and improves the efficacy of carboplatin both in cell culture and in a mouse model. Our study thus reveals the mechanistic link between ARID1A/PIK3CA mutations and cytokine gene induction in OCCC and suggests that NF-κB inhibition could be a potential therapeutic option.

INTRODUCTION

Ovarian clear cell carcinoma (OCCC) constitutes ∼10%–15% of all ovarian cancers (Jones et al., 2010). OCCC is regarded as one of the most aggressive cancers because it is generally refractory to conventional chemotherapies such as Taxol or cisplatin (Bast et al., 2009). Genome sequencing of OCCC patient samples has revealed highly recurrent loss-of-function mutations in ARID1A (Jones et al., 2010; Wiegand et al., 2010), a core subunit of the SWItch (SWI)/sucrose non-fermentable (SNF) ATP-dependent chromatin-remodeling complex (Wilson and Roberts, 2011). Interestingly, ARID1A mutations often co-exist with activating mutations of PIK3CA,

suggesting that they may cooperate in driving OCCC development (Samartzis et al., 2013; Yamamoto et al., 2012). Indeed, Arid1a knockout/Pik3ca H1047R transgenic mice develop spontaneous OCCC, indicating that the two mutations are sufficient in initiating OCCC (Chandler et al., 2015). Previous studies have revealed that OCCC is associated with increased expression of pro-inflammatory cytokines in both human and mouse models (Chandler et al., 2015; Yamaguchi et al., 2010). Consistently, inhibition of interleukin-6 (IL-6) in cell culture reduced proliferation of OCCC cells (Chandler et al., 2015; Kumar and Ward, 2014), suggesting induction of pro-inflammatory cytokine might contribute to OCCC tumorigenesis. However, how the two mutations cooperate to induce pro-inflammatory cytokines is not clear. Understanding the molecular mechanism underlying this process could help develop strategies overcoming dysregulation of cytokines, which can serve as a potential treatment for OCCC.

Studying tumorigenesis mechanism in existing cancer cell lines is confounded by the different mutations acquired during their derivation and maintenance. To circumvent this problem, we utilized hTERT-immortalized normal human ovarian epithelial cell lines (Liu et al., 2004). By introducing ARID1A small hairpin RNA (shRNA) and PIK3CA mutations to normal human ovarian epithelial cells, we created an in vitro OCCC model. Using this model, we identified RelA nuclear factor κB (NF-κB) transcription factor to be a major factor driving cytokine induction. Mechanistically, we demonstrate that PIK3CA acts through the AKT-IKK2 pathway to release RelA from inhibitor of kappa B (IκB). In addition, disruption of ARID1A impairs the recruitment of the Sin3A histone deacetylase (HDAC) repressor complex to cytokine genes, leading to their derepression. Importantly, inhibition of NF-κB by a chemical inhibitor attenuated the in vitro and in vivo growth of double-mutant cells and improved the efficacy of carboplatin, a clinically used cisplatin derivative. Our study thus not only reveals how mutations of a signaling molecule and an epigenetic factor can cooperate to drive tumorigenesis but also raises the possibility of inhibiting the NF-κB pathway as a potential treatment for OCCC.
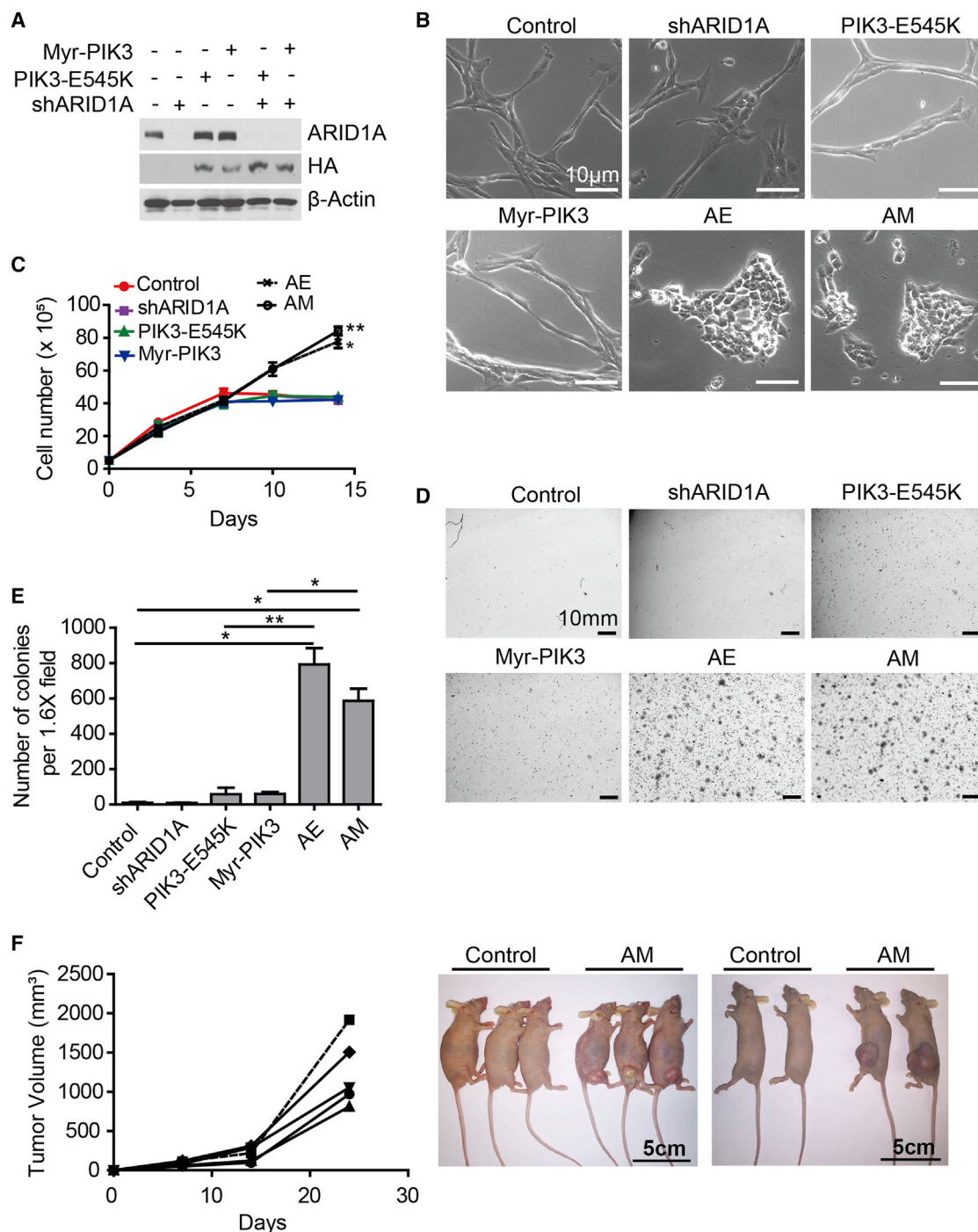
A

Myr-PIK3	-	-	-	+	-	+
PIK3-E545K	-	-	+	-	+	-
shARID1A	-	+	-	-	+	+

ARID1A

HA

β-Actin

B

Control shARID1A PIK3-E545K

Myr-PIK3 AE AM

10μm

C

- ● Control
- ■ shARID1A
- ▲ PIK3-E545K
- ▼ Myr-PIK3
- ✱ AE
- ○ AM

Cell number (× 10^5)
Days

D

Control shARID1A PIK3-E545K

Myr-PIK3 AE AM

10mm

E

Number of colonies per 1.6× field

Control, shARID1A, PIK3-E545K, Myr-PIK3, AE, AM

F

Tumor Volume (mm³)
Days

Control AM Control AM

5cm 5cm

Figure 1. ARID1A Depletion and PIK3CA Activation Transform Normal Human Ovarian Epithelial Cells

(A) Introduction of double mutations into the T80 cell line. T80 cells were transduced with retroviruses expressing an ARID1A shRNA and the indicated PIK3CA alleles. After selection, the transduced cells were analyzed by western blotting.

(B) Phase contrast images of established cell lines. Scale bar, 50 μm.

(C) Growth curve of the established T80 cell lines expressing single or double mutant. 5×10^5 of the indicated cells were plated on six-well plates and counted every 2 days (n = 3). Error bars indicate SEM. Statistical analysis comparing AM or AE cells with control cells was performed on day 14.

(D) Soft agar assay of the established T80 cell lines expressing single or double mutant. Representative images of soft agar colonies. Scale bar, 10 mm.

(E) Colony numbers per 1.6× field were counted (n = 3). Error bars indicate SEM.

RESULTS

ARID1A Depletion and PIK3CA Mutations Transform Normal Human Ovarian Epithelial Cells

To generate an in vitro model for the study of OCCC containing loss-of-ARID1A-function and gain-of-PIK3CA-function mutations, we introduced single or double mutations into the immortalized normal human ovarian epithelial cell line T80 (Liu et al., 2004) by depleting ARID1A using a shRNA and/or expressing active PIK3CA, respectively (Figure 1A). For PIK3CA, we used either PIK3CA E545K or myristoylation-signal-attached PIK3CA (Myr-PIK3CA). PIK3CA E545K is a naturally occurring mutant PIK3CA found in cancer patients that has increased enzymatic activity (Samuels et al., 2005), while Myr-PIK3CA is forcibly recruited to membrane and is constitutively active (Bitler et al., 2015). Although cells expressing ARID1A shRNA or active PIK3CA alone exhibit cell morphology similar to that of control, cells with both (hereafter AE for ARID1A shRNA and E545K and AM for ARID1A shRNA and Myr-PIK3CA) have strikingly different morphology, with smaller size and disrupted organization (Figure 1B). Although T80 (AE) and T80 (AM) cells exhibited an initial growth rate similar to that of control T80 cells or cells with a single mutation, they appeared to have lost cell contact inhibition growth, as they kept growing by piling up on each other (Figure 1C). To ascertain that these observations are not due to a peculiar property of the T80 cell line, we performed similar experiments in T29, another independently established normal human ovarian epithelial cell line (Liu et al., 2004). Results shown in Figure S1 indicate that introduction of the double mutations also caused a morphological change as well as loss of contact inhibition of growth (Figures S1B and S1C).

Next, we examined the ability of T80 cells harboring the double mutations to grow in an anchorage-independent manner. To this end, soft agar assay was performed using cells with single or double mutations. Results shown in Figures 1D and 1E indicated that cells with active PIK3CA displayed a weak ability to grow in soft agar, which was drastically enhanced when combined with ARID1A depletion. Importantly, both PIK3CA mutations exhibited a similar result. To evaluate the tumorigenecity of the cells harboring the two mutations, T80 (AM) cells were subcutaneously injected into nude mice. 2 weeks after the injection, palpable tumors were observed in all mice tested (five out of five), which is in contrast with the mice injected with the same number of control T80 cells (Figure 1F). Collectively, the above results suggest that ARID1A depletion in combination with PIK3CA activation is sufficient to transform normal human ovarian epithelial cells.

ARID1A Depletion and PIK3CA Activation Induce Pro-inflammatory Cytokine Expression

To gain insight into the molecular mechanism of how combined loss of ARID1A and gain of PIK3CA function contributes to transformation of human ovarian epithelial cells, we performed tran-

scriptome analyses by RNA sequencing (RNA-seq). To this end, T80 and T29 cells, as well as their derivatives harboring single or double mutations, were used for RNA-seq analysis. Comparison of their transcriptomes revealed 59 genes uniquely upregulated in the cells harboring double mutations (fold change [FC] $\geq$ 2 in both T29 [AM] and T80 [AM] cells) (Figure 2A; Table S1). To examine if these upregulated genes are relevant to human OCCC, we performed a gene set enrichment analysis using the identified 59 genes. By analyzing an available OCCC patient gene expression dataset GSE6008 (Hendrix et al., 2006), we confirmed that the 59 genes were indeed enriched in the upregulated gene groups in OCCC patient samples (Figure 2B), supporting the relevance of the upregulation of these genes to human OCCC. Gene Ontology (GO) analysis revealed cytokine/chemokine activity as the most enriched GO term (Figure S2A). Kyoto Encyclopedia of Genes and Genomes (KEGG) pathway analysis also revealed cytokine signaling as the most enriched pathway (Figure S2B). Among the 59 genes identified, 14 belong to the pro-inflammatory cytokines, including IL-1A, IL-1B, IL-6, IL-8, CXCL1, and CXCL3 (Table S1). To confirm the RNA-seq result, we performed qRT-PCR on a subset of cytokine genes. Results shown in Figure 2C indicated that either ARID1A depletion or PIK3CA activation alone only slightly upregulated cytokine gene expression. However, the combined mutations resulted in a robust activation. Similar results were also obtained in cells harboring the AE mutations (Figure S2C). In contrast to the upregulated genes, no enrichment of any GO term or pathway was identified in the downregulated genes, suggesting that upregulation of these cytokines may underlie the molecular function of the double mutations.

The finding that double mutations result in upregulation of pro-inflammatory cytokines is intriguing. First, upregulation of certain cytokines has been previously observed in a mouse OCCC model and human OCCC patients (Chandler et al., 2015; Yamaguchi et al., 2010), suggesting its clinical relevance. Second, several of these cytokines, including IL-6, IL-8, and CXCL1, have been previously implicated in promoting cell proliferation, survival, chemoresistance, metastasis, and cancer stem cell expansion (Acharyya et al., 2012; Grivennikov et al., 2009; Iliopoulos et al., 2009; Schafer and Brugge, 2007; Waugh and Wilson, 2008). Thus, induction of these oncogenic cytokines may contribute to tumorigenesis. Consistent with a previous report that blocking IL-6 function can reduce proliferation of cancer cells harboring ARID1A/PIK3CA mutations (Chandler et al., 2015), neutralizing antibody against IL-6 was able to slow down proliferation of T80 (AM) cells, but not control T80 cells (Figure 2D). Collectively, T80 (AM) cells offer an in vitro experimental model for understanding the molecular basis of ARID1A/PIK3CA-mutation-induced OCCC.

RelA NF-κB Transcription Factor Is a Major Contributing Factor in Pro-inflammatory Cytokine Activation

Previous studies have established that the signal transducer and activator of transcription (STAT) and NF-κB transcription

---

(F) T80 cell line harboring the double mutant can form tumors in nude mice. Six-week-old female nu/nu mice were subcutaneously injected with 3×10^5 control T80 or T80 (AM) cells (two independent experiments with five mice total in each group). Tumor volume was measured every week for each mouse (left growth curve). Mice were imaged at the time of sacrifice (right). Scale bar, 5 cm.

*p < 0.05; **p < 0.01. See also Figure S1.

A

B

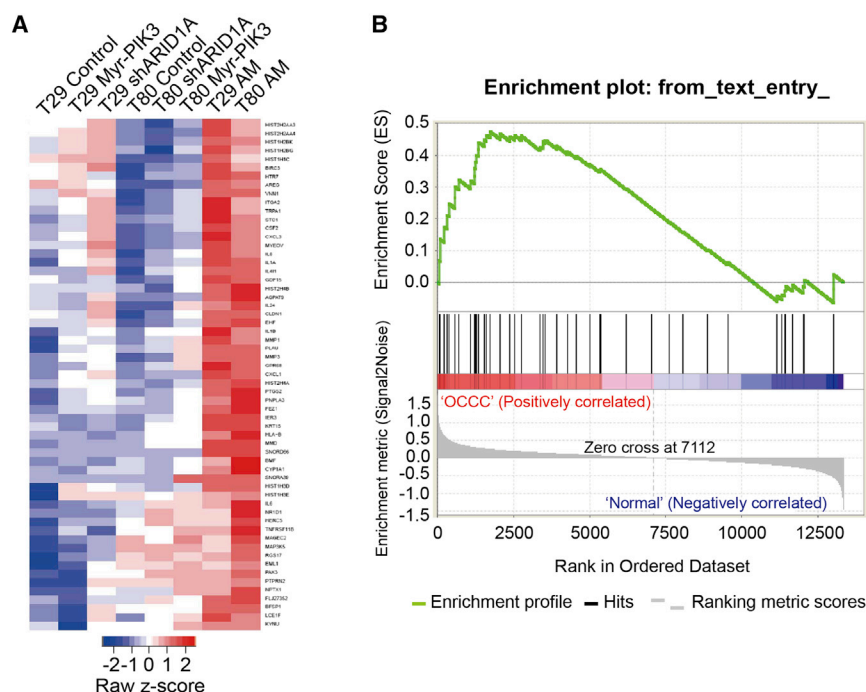Enrichment plot: from_text_entry_

Figure 2. Cytokine Genes Are Aberrantly Up-regulated in ARID1A/PIK3CA Mutant Cells

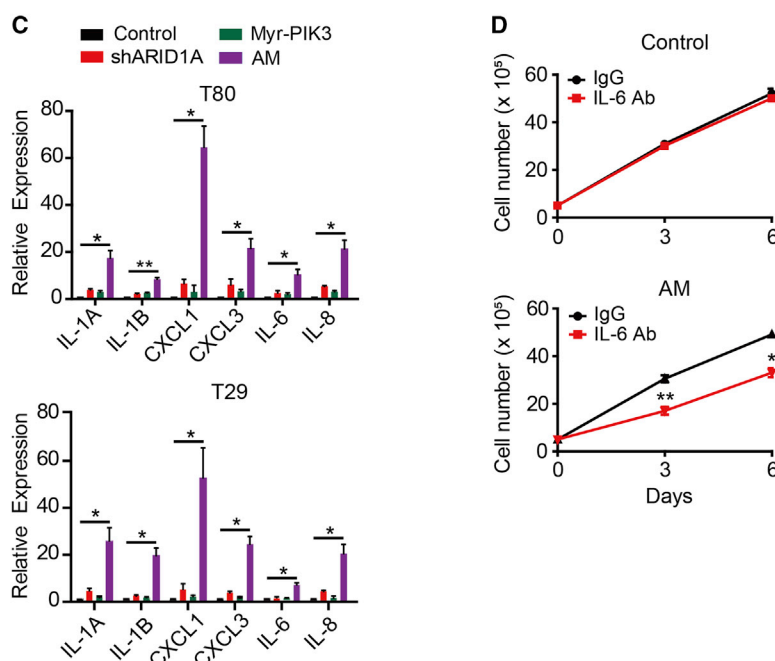(A) Heatmap of the genes commonly upregulated in T29 (AM) and T80 (AM) cells compared to all other cell lines (FC ≥ 2).

(B) Genes identified in (A) are enriched in the up-regulated genes in OCCC. Genes upregulated in patient OCCC samples relative to normal tissues (from GSE6008) were ranked from left to right, and gene set enrichment on the upregulated genes can be seen in the top and middle panels.

(C) qRT-PCR verification of the RNA-seq result. mRNA level of selected cytokines genes were validated by qRT-PCR, normalized by β-actin transcripts (n = 3 for all experiments except CXCL1 in T29, of which n = 4). Error bars indicate SEM.

(D) IL-6 antibody can partly block T80 (AM), but not T80, cell growth. Control T80 or T80 (AM) cells were incubated with anti-mouse immunoglobulin G (IgG) or IL-6 neutralizing antibody (2 ng/mL) (n = 3), and the cell proliferation rate was measured. Error bars indicate SEM.

*p < 0.05; **p < 0.01. See also Figure S2 and Table S1.

C

D

cating that cytokine gene induction in the double-mutant cell is mainly mediated through the NF-κB pathway. Given that STAT activation was observed in both a mouse OCCC model and human OCCC patients (Chandler et al., 2015; Yamaguchi et al., 2010), it was surprising that STAT inhibition did not result in cytokine gene suppression. Because STAT can be activated by cytokines (Grivennikov and Karin, 2010), our results suggest that STAT activation observed in OCCC is likely a secondary effect of NF-κB-mediated cytokine induction.

To substantiate the role of NF-κB in cytokine gene activation in the context of ARID1A/PIK3CA double mutations, we performed genetic manipulation. The NF-κB family transcription factors include both RelA and RelB that target overlapping as well as specific genes (Napetschnig and Wu, 2013; Sun, 2011). To determine whether RelA or RelB is involved in cytokine gene activation, we obtained small interfering RNAs

pathways play an important role in cytokine gene induction (Grivennikov and Karin, 2010). To examine whether the two pathways are involved in ARID1A/PIK3CA-mutation-caused cytokine induction, we treated T80 (AM) cells with either a STAT inhibitor (1 μM ruxotinilib) or an NF-κB inhibitor (1 μM IKK-IIV) and quantified cytokine expression by qRT-PCR. While ruxotinilib had no significant effect, IKK-IIV markedly reduced the expression of cytokine genes (Figure 3A), indi-

(siRNAs) that deplete RelA or RelB, respectively (Figures S3A and S3B). While RelA knockdown efficiently decreased cytokine gene expression in T80 (AM) cells, knockdown of RelB had no significant effect (Figures 3B and S3C). RelA and RelB are differentially regulated by the IKK signalosome, which consists of three core proteins, IKK1 (IKKα), IKK2 (IKKβ), and IKKγ, with IKK1 and IKK2 functioning as kinases and IKKγ serving as a regulatory subunit. In response to signals that activate IKK2,
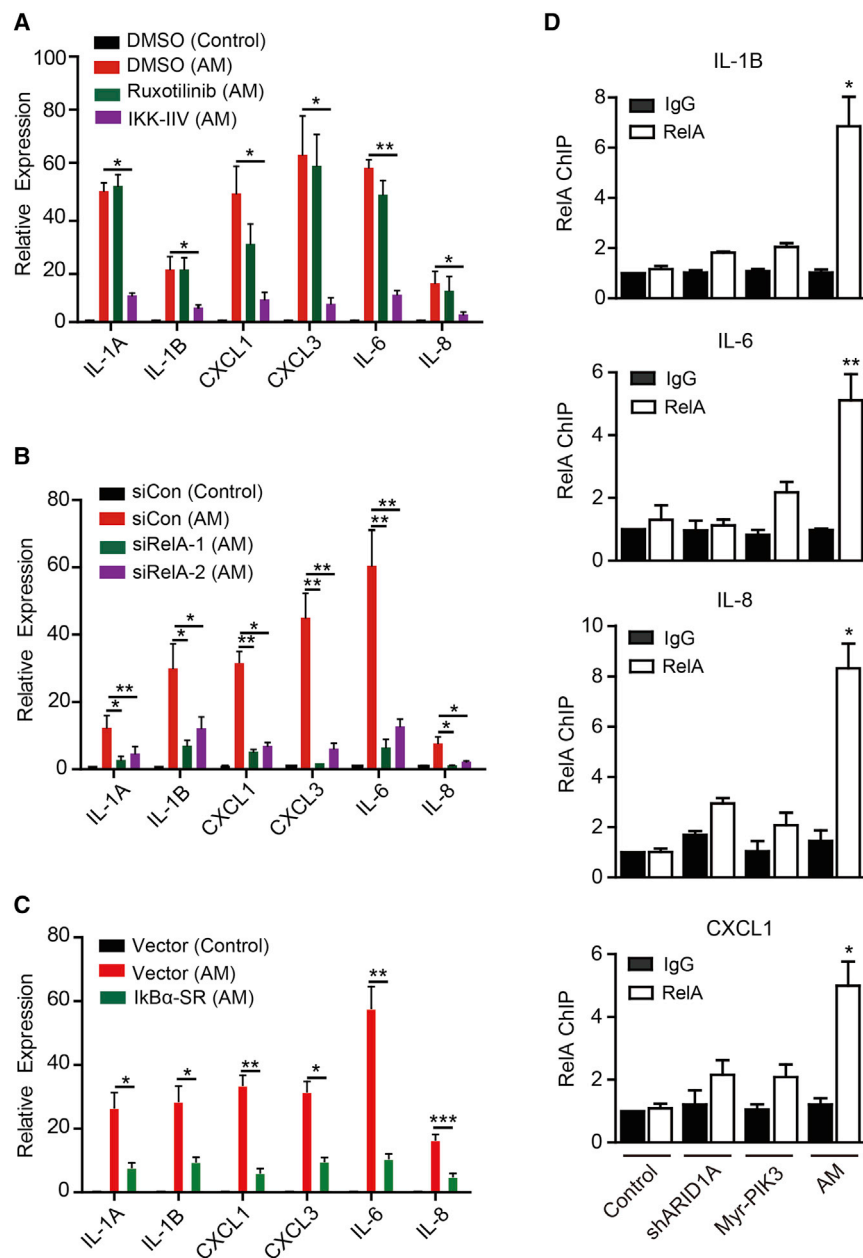
A

Relative Expression

- DMSO (Control)
- DMSO (AM)
- Ruxotilinib (AM)
- IKK-IIV (AM)

IL-1A IL-1B CXCL1 CXCL3 IL-6 IL-8

B

Relative Expression

- siCon (Control)
- siCon (AM)
- siRelA-1 (AM)
- siRelA-2 (AM)

IL-1A IL-1B CXCL1 CXCL3 IL-6 IL-8

C

Relative Expression

- Vector (Control)
- Vector (AM)
- IκBα-SR (AM)

IL-1A IL-1B CXCL1 CXCL3 IL-6 IL-8

D

RelA ChIP

IL-1B

IL-6

IL-8

CXCL1

- IgG
- RelA

Control shARID1A Myr-PIK3 AM

Figure 3. The RelA NF-κB Transcription Factor Is Required for Cytokine Gene Activation in ARID1A/PIK3CA Mutant Cells

(A) The NF-κB inhibitor IKK-IIV, but not the STAT inhibitor ruxotinilib, inhibited cytokine expression in T80 (AM) cells. T80 (AM) cells were treated with DMSO, ruxotinilib (1 μM) or IKK-IIV (1 μM) for 3 days. Control cells were treated with DMSO. Expression of selected cytokines genes was measured by qRT-PCR, normalized by β-actin (n = 3). Error bars indicate SEM.

(B) RelA knockdown reduced cytokine gene expression. Control and T80 (AM) cells were transfected as indicated and the expression of selected cytokines genes were analyzed by qRT-PCR 3 days after transfection (n = 4). Error bars indicate SEM.

(C) RelA inhibition by a dominant-negative IκB partly reduced cytokine gene expression. T80 (AM) cells were infected with empty or IκBα-SR expression retrovirus vector. After selecting with 100 ng/mL Zeocin for 2 days, surviving cells were analyzed by qRT-PCR (n = 4). Error bars indicate SEM.

(D) Cytokine genes are direct RelA targets. ChIP analysis was performed in the indicated cells using antibodies against rabbit IgG (control) or RelA. Immunoprecipitated samples were PCR amplified using primers that amplify the RelA elements of the indicated genes. The signals were normalized with input (n = 3). IgG of control cells was set as 1. Error bars indicate SEM. Statistical analysis comparing RelA ChIP in AM and control cells is presented.

$p < 0.05$; $p < 0.01$; $p < 0.001$. See also Figure S3.

IKK2 phosphorylates IκB, leading to its degradation, which then frees RelA from IκB-mediated cytoplasmic sequestration (Mercurio et al., 1997; Xia et al., 2014). To confirm RelA-mediated cytokine induction is part of the IKK signaling, we used a dominant-negative IκBα, IκBα-SR, which carries two serine-to-alanine mutations in IKK2 target sites and thus can block IKK2 signaling when overexpressed (Brown et al., 1995). Results shown in Figure 3C indicate that expression of IκBα-SR in T80 (AM) cells successfully reduced cytokine gene expression. We note that IKK-IIV, IκBα-SR, or RelA depletion did not completely suppress cytokine gene expression to the level of control cells. This is likely due to the existence of additional factors contributing to cytokine expression. Nevertheless, our re-

sults using multiple approaches indicate that RelA does play a major role in driving cytokine gene expression in the ARID1A/PIK3CA double mutant T80 (AM) cells. Importantly, RelA appears to directly contribute to cytokine gene upregulation, as chromatin immunoprecipitation (ChIP) qPCR analysis demonstrates that RelA's occupancy at the NF-κB binding elements of IL-6, IL-8, IL-1B, and CXCL1 genes is significantly increased in T80 (AM) cells compared to other control cells (Figure 3D).

The PIK3CA-AKT-IKK2 Pathway Releases RelA from IκB

We next attempted to establish a link between PIK3CA activation and RelA-mediated cytokine gene activation. Previous studies in Jurkat cells or human fibroblasts have indicated that AKT, the main downstream target of PIK3CA, can free RelA from IκB by regulating IKK2 (Kane et al., 1999; Romashkova and Makarov, 1999). To examine whether a similar relationship exists in human ovarian epithelial cells, we introduced PIK3CA activation (Myr-) and ARID1A knockdown in T80 cells. While Myr-PIK3CA expression reduced IκB and increased phospho-IκB levels, ARID1A
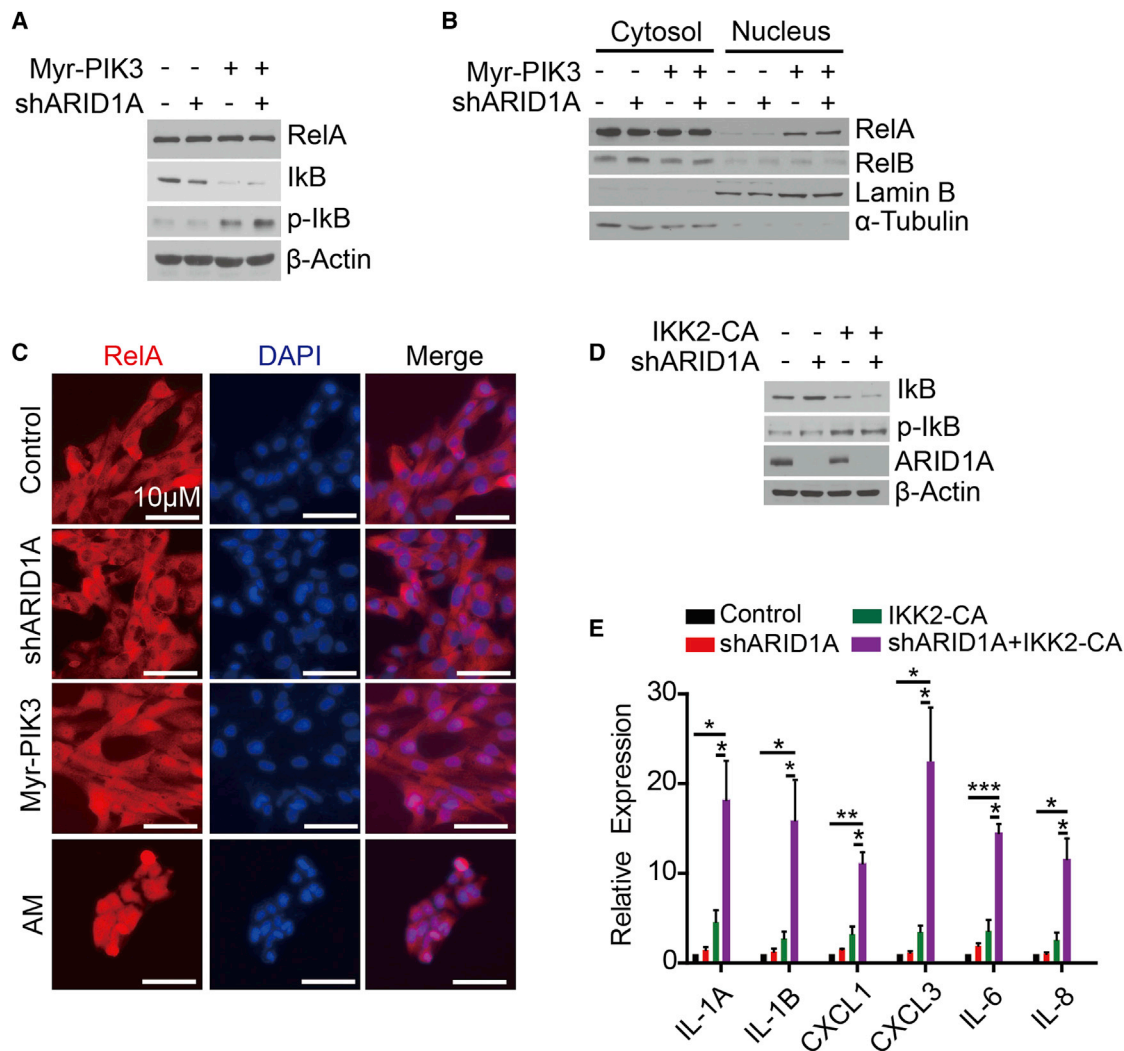
Figure 4. Active PIK3CA Releases RelA from IκB through the AKT-IKK2 Pathway

(A) PIK3CA leads to IκB phosphorylation. Western blot analysis of total and phosphorylated IκB in T80 cells expressing shARID1A, Myr-PIK3CA, or a combination. β-actin serves as a loading control.

(B) PIK3CA leads to nuclear localization of RelA. The indicated cells were fractionated to cytoplasm and nucleus and analyzed by western blotting for RelA and RelB. Lamin B and α-tubulin were used as nuclear and cytoplasmic markers, respectively.

(C) Nuclear localization of RelA in PIK3CA cells. Immune staining of RelA in the indicated cells co-stained with DAPI. Scale bar, 10 μm.

(D) IKK2-CA can replace PIK3CA in mediating IκB phosphorylation. T80 cells were transduced with retroviruses expressing ARID1A shRNA or IKK2-CA or in combination. Total and phosphorylated IκB levels were analyzed by western blotting.

(E) IKK2-CA causes cytokine gene activation. Cells from (D) were analyzed by qRT-PCR for the indicated cytokine genes, normalized by β-actin transcripts (n = 4). Error bars indicate SEM. *p < 0.05; **p < 0.01; ***p < 0.001.

See also Figure S4.

knockdown had no effect on IκB status (Figure 4A). Consistently, Myr-PIK3CA expression increased nuclear amount of RelA, but not RelB, as judged by western blotting (Figure 4B), which was further supported by immunostaining (Figure 4C).

To test whether AKT is a downstream effector of ARID1A/PIK3CA double-mutation-mediated cytokine induction, we treated T80 (AM) cells with MK-2206, an AKT-specific inhibitor. MK-2206 treatment not only restored IκB levels (Figure S4A) but also suppressed cytokine induction (Figure S4B), indicating AKT is an integral component of the

ARID1A/PIK3CA-mediated cytokine induction pathway. If the PIK3CA-AKT pathway releases RelA from IκB through IKK2, then constitutively active IKK2 (IKK2-CA) should be able to replace PIK3CA. To test this hypothesis, we established cell lines expressing IKK2-CA with or without ARID1A shRNA (Figure 4D). We found that cells with both IKK2-CA and ARID1A shRNA robustly induced cytokine gene expression (Figure 4E). This result, together with the fact that the IKK inhibitor abolishes cytokine expression (Figure 3A), allowed us to conclude that the functional effect of PIK3CA mutation in activation of

cytokines is to release RelA from IκB through the AKT-IKK2 pathway.

ARID1A Recruits the Sin3A-HDAC Complex to Cytokine Genes

We next attempted to understand how loss of ARID1A function contributes to RelA-mediated cytokine gene induction. Since ARID1A is a component of the SWI/SNF ATP-dependent remodeling factor, we first considered the possibility that loss of ARID1A might affect chromatin accessibility by RelA, thus changing RelA-mediated cytokine gene expression. To address this possibility, we performed DNaseI hypersensitivity site (DHS) analysis by DNaseI hypersensitive sites sequencing (DNase-seq) (Neph et al., 2012). Consistent with the known function of the SWI/SNF complex in facilitating chromatin access, depletion of ARID1A resulted in loss of 153 (control versus ARID1A shRNA, FC ≥ 3) and 557 (Myr-PIK3CA versus AM, FC ≥ 3) DHSs, respectively (Figure S5A). However, neither ARID1A shRNA alone nor ARID1A/PIK3CA double mutations generated new or increased DHS signal (FC ≥ 3), including the genomic regions of the altered cytokine genes (Figure S5B). Thus, increased cytokine expression in T80 (AM) cells is not likely due to increased RelA accessibility to the cytokine genes. The lack of a significant effect of loss ARID1 function on the cytokine gene accessibility by RelA is likely due to the fact that the RelA binding sites are already accessible in control cells (Figure S5B, red bars).

After ruling out the possibility that ARID1A depletion contributes to cytokine induction through regulating chromatin accessibility, we explored alternative mechanisms. Although the SWI/SNF complex is mostly involved in gene activation, it can also repress transcription by recruiting histone deacetylase complexes (Harikrishnan et al., 2005; Zhang et al., 2000). It is possible that ARID1A depletion may affect HDAC complex recruitment, leading to derepression of cytokine gene expression. Before testing if ARID1A recruits the Sin3A-HDAC complex to the cytokine genes, we first demonstrated that ARID1A does bind to the promoters of IL-6 and IL-8 genes in T80 cells by ChIP assays (Figures 5A and 5B). We then asked whether the histone acetylation status at the ARID1A binding sites is affected by ARID1A depletion. ChIP analysis using a pan-H4 acetylation antibody revealed that knockdown of ARID1A in T80 (AM) cells resulted in an increase in histone acetylation at the IL-6 and IL-8 promoters (Figure 5C). Consistently, HDAC1 binding to these regions was lost in response to ARID1A knockdown, but not to PIK3CA activation (Figure 5D), supporting a role of ARID1A in the recruitment of HDAC1 to these gene promoters.

To examine whether the enzymatic activity of the recruited HDAC is involved in suppressing cytokine gene expression, we tested the effect of the HDAC inhibitor, trichostatin A (TSA). Remarkably, TSA treatment greatly induced cytokine gene expression in cells expressing Myr-PIK3CA (Figure 5E) but only modestly induced cytokine gene expression in control cells, indicating a synergistic effect between HDAC inhibition and PIK3CA activation in cytokine induction. We further demonstrated that the HDAC1 involved is part of the Sin3A complex, as depletion of Sin3A by siRNAs, similar to that of HDAC inhibition, was able to synergize with Myr-PIK3CA to induce cytokine expression (Figures 5F and S6). Interestingly, a recent study indicated

that ARID1A can recruit the Sin3A-HDAC complex to the telomerase gene in ovarian cancer (Suryo Rahmanto et al., 2016). Collectively, these results support the notion that ARID1A recruits the Sin3A-HDAC complex to suppress cytokine gene expression. Thus, loss of ARID1A can synergize with RelA activated by PIK3CA.

The Mechanism of Cytokine Gene Activation Is Conserved in Human OCCC Cells

Having established the mechanism of cytokine gene activation in the T80 cell line model, we next asked whether this mechanism is also used for cytokine gene activation in patient-derived OCCC cell lines. To this end, two OCCC cell lines (TOV-21G, which carries both ARID1A and PIK3CA mutations, and ES-2, which does not harbor mutation on either ARID1A or PIK3CA) were used to address the question. Similar to the results obtained in T80, TOV-21G cells had decreased IκB expression and increased phospho-IκB expression compared to ES-2 cells (Figure 6A). Consistently, nuclear RelA expression was higher in TOV-21G cells compared to that in ES-2 cells, as judged by both cell fractionation and immune staining (Figures 6B and 6C). Additionally, IKK-IIV effectively decreased cytokine gene expression in TOV-21G cells, but not in ES-2 cells (Figure 6D). Furthermore, siRNA-mediated depletion of RelA decreased cytokine gene expression in TOV-21G cells, but not in ES-2 cells (Figure 6E). ChIP-qPCR analysis confirmed that RelA binds to cytokine genes in TOV-21G cells, but not in ES-2 cells (Figure 6F). Finally, we analyzed histone acetylation status and HDAC1 recruitment and found that histone acetylation is increased and HDAC1 recruitment is decreased in TOV-21G cells relative to that in the ES-2 cells, respectively (Figures 6G and 6H). Collectively, these results demonstrate that the mechanism used for cytokine induction in T80 (AM) cells is conserved in the human OCCC TOV-21G cell line.

NF-κB Inhibitor Attenuates Growth of ARID1A and PIK3CA Mutant Cells and Improves the Efficacy of Carboplatin

The fact that a PIK3CA activating mutation caused cytokine activation through RelA raises the possibility that NF-κB inhibitors could be used as a novel therapy for OCCC with ARID1A and PIK3CA mutations. Pro-inflammatory cytokines have been previously implicated in several aspects of tumorigenesis, including cell proliferation and survival and in conferring resistance to chemotherapy, especially cisplatin (Acharyya et al., 2012; Grivennikov et al., 2009; Iliopoulos et al., 2009; Schafer and Brugge, 2007). Therefore, we thought that an NF-κB inhibitor may attenuate cell proliferation and improve the efficacy of cisplatin through suppression of cytokine gene activation. The latter effect is particularly relevant given that OCCC is known to be cisplatin resistant (Bast et al., 2009). To this end, we first tested the effect of an NF-κB inhibitor on cell proliferation and found that while the proliferation rate of control cells or cells with a single mutation was not affected, growth of T80 (AM) cells was partly attenuated by the NF-κB inhibitor IKK-IIV (Figure 7A, black and purple curves). The partial attenuation might be due to either a partial rescue of cytokine gene expression by IKK-IIV or a limited contribution of cytokines to cell proliferation. Interestingly, when cells
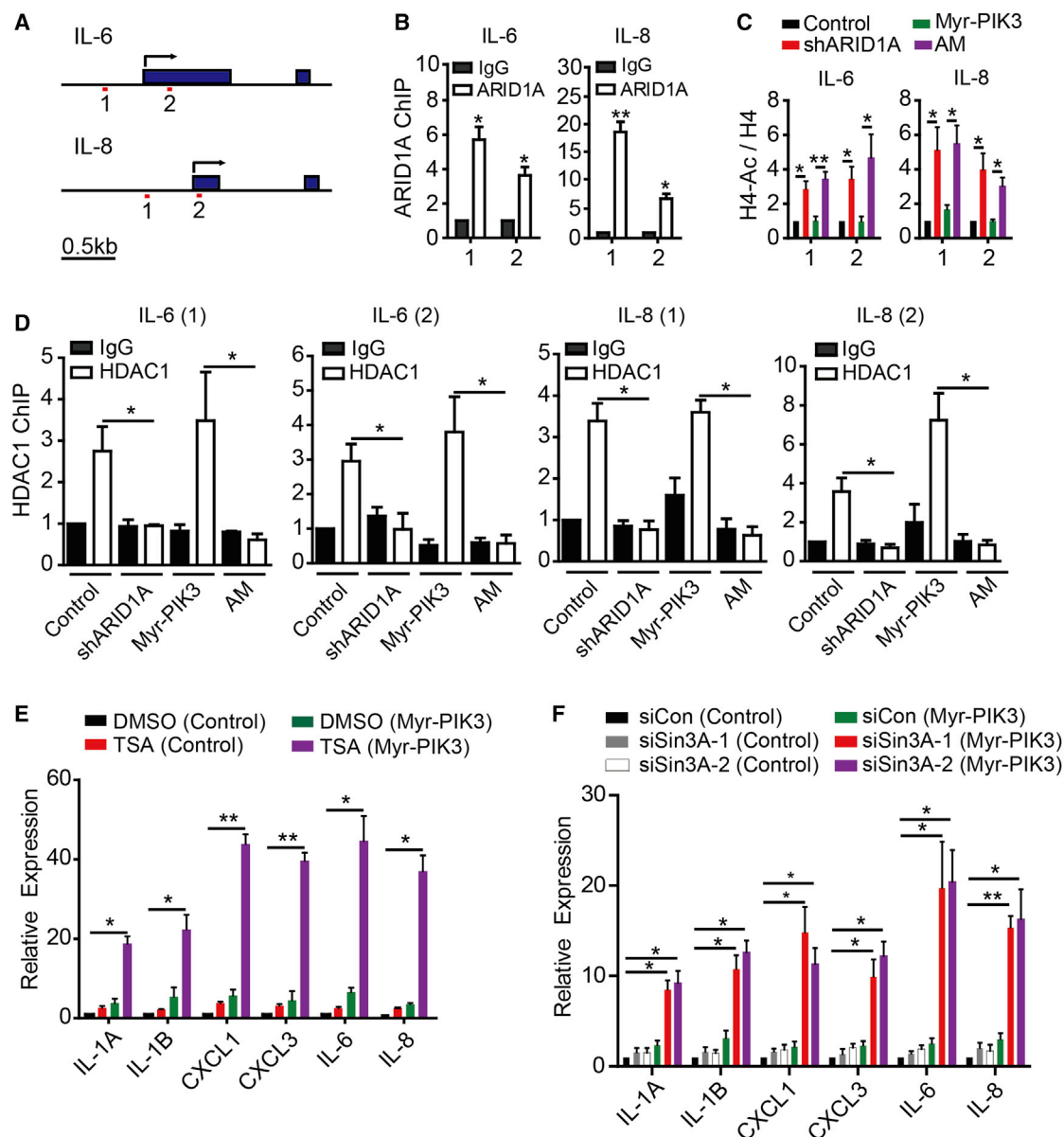
Figure 5. ARID1A Suppresses Cytokine Gene Expression by Recruiting the Sin3A-HDAC Complex

(A) Schematic diagrams of the IL-6 and IL-8 gene loci for ChIP analysis. Transcription start sites (TSSs) are indicated by arrows. Filled boxes indicate exons. The two amplicons at promoter regions are indicated. Scale bar, 0.5 kb.

(B) ARID1A binds to IL-6 and IL-8 promoters. T80 cells were subjected to chromatin immunoprecipitation (ChIP) using an antibody against IgG or ARID1A. The amplicons are indicated in (A), and the signals are normalized by input (n = 3). Error bars indicate SEM.

(C) ARID1A knockdown results in increased histone acetylation. The indicated T80 cells were subjected to ChIP analysis using an H4 or a pan-acetylated H4 antibody. ChIP samples were PCR amplified using the indicated primers. Acetylated H4 was normalized by H4. For each amplicon, control cell was set to 1 (n = 4). Error bars indicate SEM.

(D) Loss of HDAC1 recruitment in ARID1A knockdown T80 cell lines. Indicated T80 cells were subjected to ChIP analysis using antibodies against IgG or HDAC1. ChIP samples were PCR amplified using indicated primers, normalized by input (n = 3 for all experiments except TSS in IL-8, of which n = 4). IgG in control cells was set as 1. Error bars indicate SEM.

(E) Histone deacetylase activity is required for suppressing cytokine gene expression. The indicated cells were treated with DMSO or TSA (100 nM) for 2 days and analyzed by qRT-PCR of selected cytokines, normalized by β-actin (n = 3). Error bars indicate SEM.

(F) Sin3A depletion resulted in derepression of cytokine genes. Control or Myr-PIK3CA T80 cells were transfected with the indicated siRNAs. 3 days after transfection, cells were analyzed by qRT-PCR (n = 4). Error bars indicate SEM.

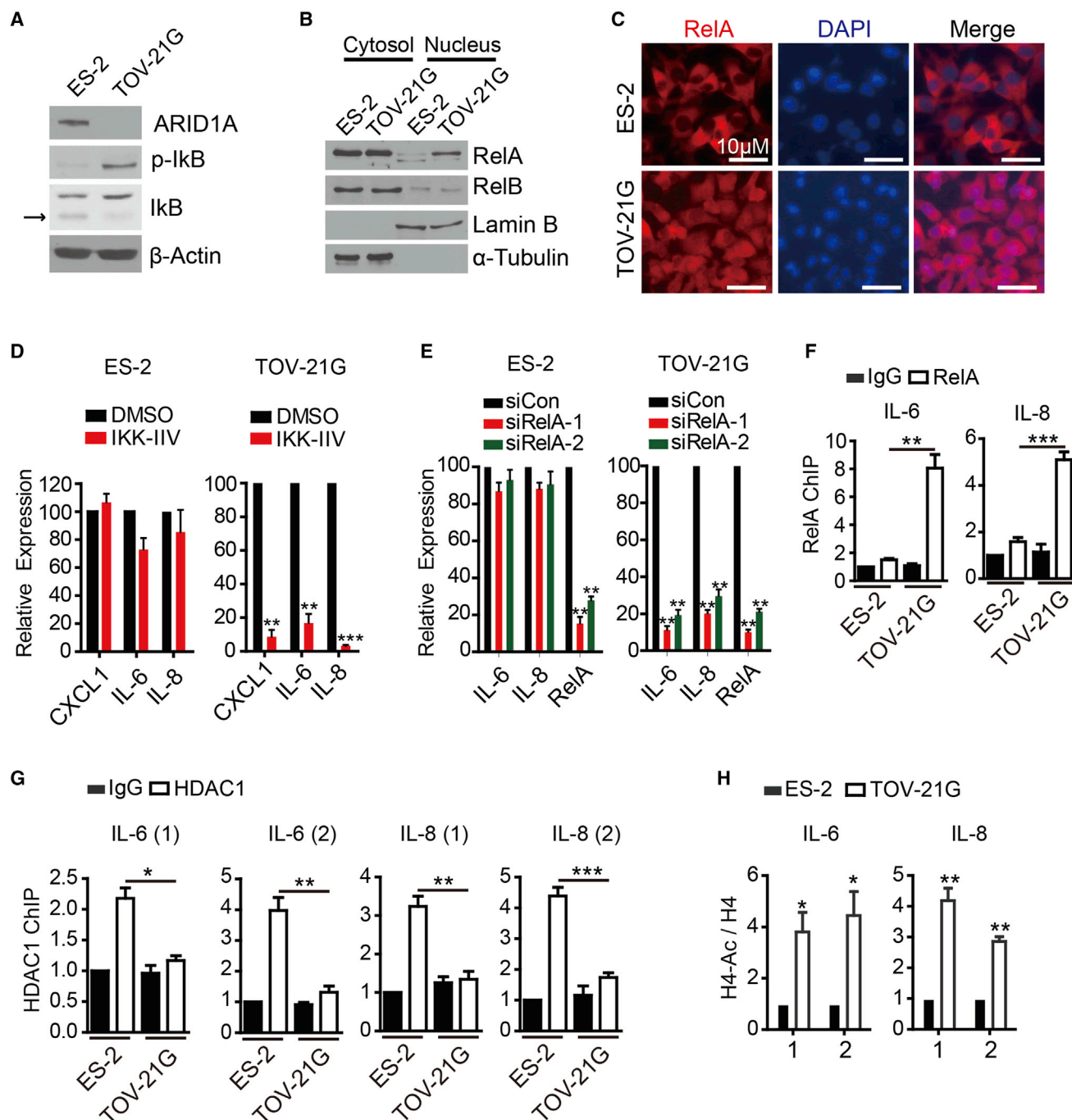*p < 0.05; **p < 0.01. See also Figure S6.

Figure 6. Mechanism of Cytokine Gene Activation Is Conserved in a Human OCCC Cell Line

(A) The phosphorylation state of IκB in ARID1A/PIK3CA mutant and wild-type OCCC cell lines. ES-2 (wild-type) and TOV-21G (double mutant) cell lysates were analyzed by western blotting using the indicated antibodies. Arrow points to IκB.

(B) RelA is localized in nucleus in TOV-21G cell. ES-2 and TOV-21G cells were fractionated to the cytoplasm and nucleus and analyzed by western blot with RelA and RelB antibodies.

(C) Nuclear localization of RelA in TOV-21G cells, and immune staining of RelA in the indicated cells co-stained with DAPI. Scale bar, 10 μm.

(D) The NF-κB inhibitor IKK-IIV suppresses cytokine gene expression in the TOV-21G, but not in the ES-2, OCCC cell line. Cells were treated with DMSO or IKK-IIV (1 μM) for 3 days. Their effect on cytokine gene expression was analyzed by qRT-PCR (n = 3).

(E) RelA knockdown suppresses cytokine gene expression in the TOV-21G, but not in the ES-2, OCCC cell line. Cells were transfected as indicated, and the expression of selected cytokine genes was analyzed by qRT-PCR 3 days after transfection (n = 4). Error bars indicate SEM.

(legend continued on next page)

were treated with carboplatin, a clinically used derivative of cisplatin, only T80 (AM) cells showed persistent growth, while the growth of other cells was effectively arrested (Figure 7A, green curves). Importantly, when carboplatin was combined with IKK-IIV, growth of T80 (AM) cells was also arrested (Figure 7A, red curves). Of note, recombinant IL-6 and IL-8 was able to rescue this effect (Figure S7), indicating that IL-6 and IL-8 activation is mainly responsible for the chemoresistant effect. Consistent with its effect on T80 (AM) cells, IKK-IIV partially attenuated proliferation of TOV-21G cells, but not that of the ES-2 cells (Figure 7B, black and purple curves). Importantly, when combined with carboplatin, IKK-IIV completely arrested TOV-21G cell proliferation (Figure 7B, red curves).

To examine whether the combined therapy is also effective in vivo, we transplanted TOV-21G cells into nude mice by subcutaneous injection. When the tumors reached palpable size ($\sim$100 mm^3), we divided the mice into four groups randomly and subjected them to the following treatment: saline control, carboplatin only (30 mg/kg, once per week), IKK-IIV only (25 mg/kg, twice per week), and carboplatin plus IKK-IIV, respectively. While single treatments showed partial attenuation of tumor growth, combined treatment completely arrested tumor growth (Figures 7C and 7D). These results demonstrate that the NF-κB inhibitor IKK-IIV is able to selectively suppress proliferation of ARID1A/PIK3CA double-mutant cells and has the potential to improve the efficacy of carboplatin in OCCC treatment.

DISCUSSION

Understanding the molecular mechanisms underlying uncontrolled cellular proliferation resulting from cancer initiating mutations is critical for developing effective treatment. Despite the identification of a large number of epigenetic factor mutations in various cancers, how these mutations contribute to tumorigenesis is poorly understood. Here, we report how a loss-of-function mutation in an epigenetic factor (ARID1A) synergizes with a gain-of-function mutation in a signaling factor (PIK3CA) to contribute to tumorigenesis in OCCC through inducing pro-inflammatory cytokine gene expression (Figure 7E). Mechanistically, loss of ARID1A releases cytokine genes from Sin3A-HDAC-mediated repression, while activating mutation of PIK3CA frees RelA from IκB so that RelA can enter the nucleus to activate cytokine genes. These mechanistic insights prompted us to test the therapeutic potential of an NF-κB inhibitor in combination with carboplatin, which is supported by our data presented in Figure 7. Our results thus provide the missing mechanistic link between ARID1A/PIK3CA mutations and cytokine gene induction.

Loss of Sin3A-HDAC Repression Underlies Cytokine Gene Induction in OCCC

Components of the SWI/SNF complex, including ARID1A, are frequently mutated in different types of cancers (Kadoch and Crabtree, 2015). Understanding how these mutations contribute to oncogenesis is of great importance. Although the DNaseI accessibility to the cytokine genes is not altered by loss of ARID1A, the recruitment of the Sin3A-HDAC complex to cytokine genes is impaired by loss of ARID1A. HDAC1 and HDAC2 exist in at least two distinctive protein complexes that include nucleosome remodeling and deacetylase (NuRD) and Sin3A (Zhang et al., 1997, 1998). The NuRD complex has established function in cancer (Lai and Wade, 2011; Wang et al., 2009). Therefore, HDAC inhibitors have been widely used as anticancer drugs with promising outcomes (Minucci and Pelicci, 2006). In contrast, the role of the Sin3A-HDAC complex in cancer has been unclear. Interestingly, our results indicate that the Sin3A-HDAC complex serves as a tumor suppressor in OCCC. Consistent with the fact that an HDAC inhibitor failed to show beneficial effects in cisplatin-resistant ovarian cancers in a phase 2 clinical trial (Mackay et al., 2010), our results suggest that HDAC inhibitors would not be effective for OCCC and could even cause unfavorable outcomes.

An unanswered but important remaining question is whether the chromatin-remodeling function of ARID1A contributes to OCCC development. It is hard to imagine that recruitment of the Sin3A-HDAC complex is the sole function of ARID1A contributing to OCCC. Future studies analyzing the relationship between transcriptional changes and DNase I sensitivity changes may reveal additional ARID1A functions. It is likely that the combined effect of chromatin-remodeling-dependent and independent functions of ARID1A contribute to oncogenesis in OCCC.

Gain of RelA Activation Drives Aberrant Cytokine Gene Induction in OCCC

The NF-κB pathway plays a central role in cancer biology through activating multiple genes involved in cell proliferation, survival, drug resistance, angiogenesis, and metastasis (Baud and Karin, 2009; Karin et al., 2004). Thus, NF-κB inhibition has been reported to increase the efficacy of several anticancer reagents (Nakanishi and Toi, 2005). However, the role of NF-κB in OCCC has been poorly characterized. Our results suggest that the RelA NF-κB transcription factor has an important role in OCCC development and progression. Constitutive activation of NF-κB has been observed in many types of cancers, especially hematological cancers (Horie, 2013). In these tumors, NF-κB is usually activated by mutations of genes that directly regulate NF-κB. Constitutive NF-κB activity is also found in some solid tumors, where NF-κB is usually activated by inflammatory cues (e.g., smoking or intestinal inflammation)

(F) RelA binds at IL-6 and IL-8 promoters in TOV-21G cells. ChIP analysis was performed using antibodies against rabbit IgG (control) or RelA. The signals were normalized to input (n = 4). IgG of control cells was set as 1. Error bars indicate SEM.

(G) HDAC1 binding at IL-6 and IL-8 is decreased in TOV-21G cells. ChIP analysis was performed using antibodies against IgG or HDAC1 and processed as (F). Error bars indicate SEM.

(H) Histone acetylation at IL-6 and IL-8 promoters is decreased in TOV-21G cells. ChIP analysis was performed using an H4 (for normalization) or a pan-acetylated H4 antibody. For each amplicon, the control cell was set to 1 (n = 4). Error bars indicate SEM.
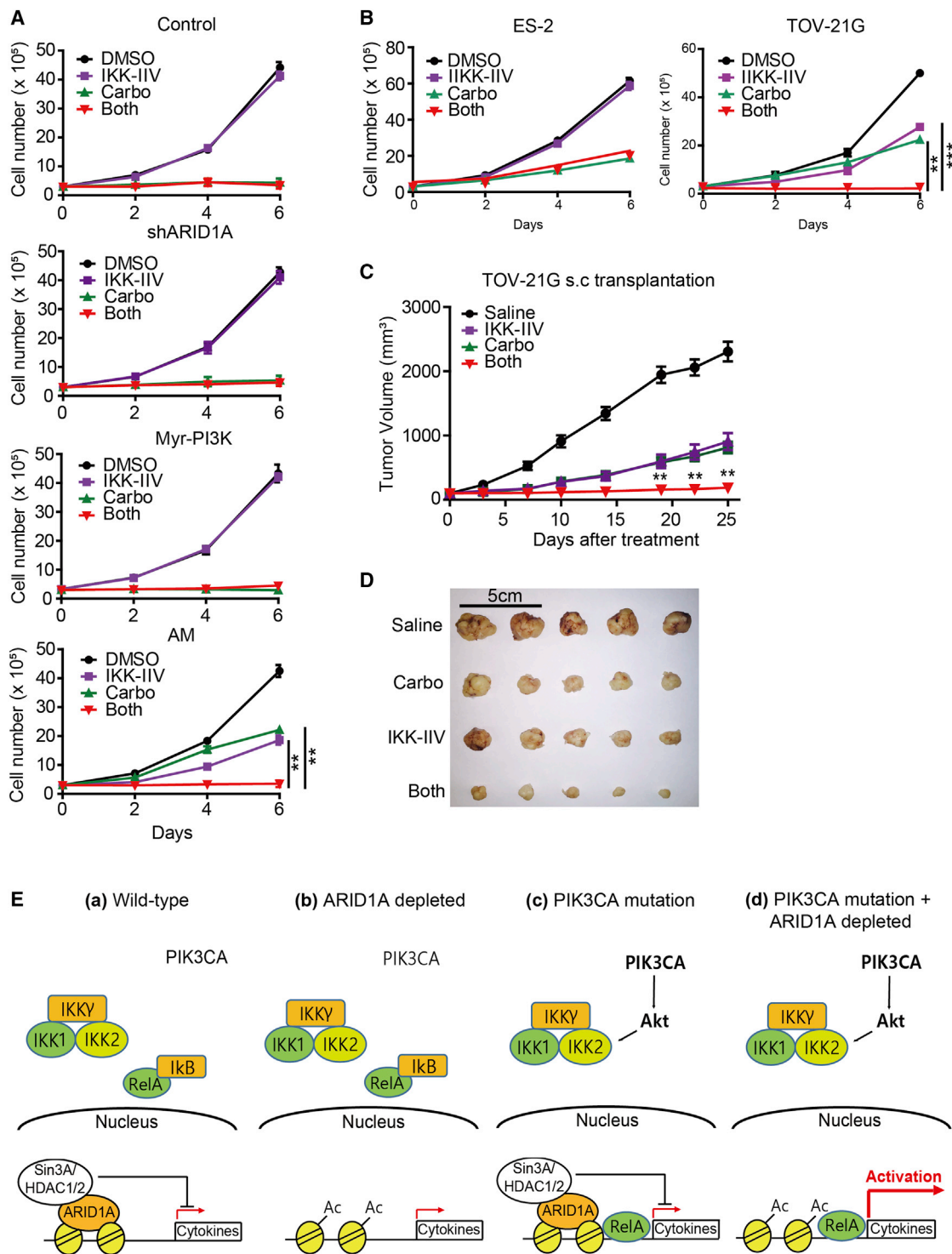
*p < 0.05; **p < 0.01.

Figure 7. NF-κB Inhibitor Suppresses Proliferation of ARID1A/PIK3CA Mutant Cells and Synergizes with Carboplatin

(A) The NF-κB inhibitor synergizes with carboplatin to suppress T80 (AM) cell proliferation. 3×10^5 of the indicated cells were plated on six-well plates. 1 day after seeding, cells were treated with the indicated drugs and counted every 2 days (n = 3). Error bars indicate SEM.

(B) Synergistic effect of IKK-IIV and carboplatin in suppressing TOV-21G, but not ES-2, cell proliferation. Cells were assayed as in (A) (n = 3). Error bars indicate SEM.

(C) Combined treatment of IKK-IIV and carboplatin inhibits TOV-21G tumor growth in a mouse xenograft model. 3×10^6 TOV-21G cells were subcutaneously transplanted to 6-week-old female nude mice and housed until tumors reached a palpable size of ~100 mm³. Mice were randomized into four groups for the

(legend continued on next page)

(Grivennikov et al., 2009; Schwitalla et al., 2013; Takahashi et al., 2010). Unlike these known NF-κB activation mechanisms, OCCC uses a unique strategy to activate NF-κB. In OCCC, a combination of two mutations that respectively derepress chromatin and activate a transcription factor contribute to cytokine gene activation. It is important to note that upregulation of pro-inflammatory cytokines in OCCC is achieved cell autonomously by the two mutations without the involvement of any environmental factors.

Potential Histone Acetyltransferases that Activate Cytokines in OCCC

Our current study did not identify the responsible histone acetyltransferases (HATs) cooperating with RelA in OCCC. So far, two HATs have been implicated in NF-κB-mediated cytokine transcription. The first is p300/CBP, which has been implicated in cytokine induction in tumor necrosis factor (TNF-α)-stimulated human umbilical vein endothelial cells (HUVEC) and leukemia cells (Gerritsen et al., 1997; Perkins et al., 1997). The second is Tip60, which has also been implicated in cytokine induction in TNF-α-stimulated HepG2 cells (Kim et al., 2012). To explore whether the two HATs are involved in cytokine gene induction in OCCC, we treated both T80 (AM) and TOV-21G cells with an inhibitor of p300 (C636) or Tip60 (Nu9056) or their combination. However, none of these treatments reduced cytokine gene expression (M.K., unpublished data). In addition, despite multiple attempts, we failed to detect binding of p300 or Tip60 at cytokine gene promoters in T80 (AM) cells. Thus, it is likely that HATs other than p300 or Tip60 may be involved in cytokine gene induction in OCCC. Identification of the responsible HAT may provide a target for OCCC treatment.

NF-κB Inhibitor as a Potential Therapeutic Option for ARID1A/PIK3CA Mutant Cancers

Our results show that NF-κB inhibition could selectively inhibit the growth of ARID1A/PIK3CA mutant cells while leaving normal cells or OCCC without these mutations unaffected. In addition, we demonstrate both in cell culture and using a mouse model that NF-κB inhibition potentiates the effect of carboplatin, which is currently the first line of treatment for ovarian cancer but is not effective for OCCC. Furthermore, cytokines upregulated in our system are implicated in cancer-stromal interaction, which can drive processes involved in cancer progression such as angiogenesis (e.g., IL-8) (Waugh and Wilson, 2008) and metastasis (e.g., CXCL1) (Acharyya et al., 2012). Therefore, we expect that NF-κB inhibition could also benefit OCCC treatment by blocking cancer progression. It would be informative to test this hypothesis in a genetically engineered mouse model of OCCC in the future. Additionally, the use of an NF-κB inhibitor would be a better strategy than suppressing expression of a specific cytokine. It is worth noting that a recent study revealed combined mutations of ARID1A/PIK3CA in gastric adenocarcinoma (Zang et al., 2012). It would be interesting to test if our findings in OCCC can also be applied to this type of gastric cancer.

EXPERIMENTAL PROCEDURES

Mouse Xenograft Assay

All animal studies were performed in accordance with guidelines of the Institutional Animal Care and Use Committee at Harvard Medical School. Six-week-old female nude mice were purchased from Jackson Laboratory (stock no. 002019, homozygous for Foxn). 3×10^6 cells (mixed with 50% Matrigel, Corning) were subcutaneously injected into the right part of back skin. Tumor sizes were measured using an electronic caliper. For treatment experiments, tumors were grown until they reached palpable size of ~100 mm³. Then, mice were randomized into four groups and treated with saline, carboplatin only (30 mg/kg, once per week), IKK-IIV only (25 mg/kg, twice per week), or a combination by intraperitoneal injection.

RNA-Seq

RNA-seq libraries were made from poly(A)+ mRNA using NEBNext Ultra Directional RNA Library Prep Kit for Illumina (New England Biolabs). Briefly, mRNA was purified from 1 μg total RNA using NEBNext Poly(A) mRNA Magnetic Isolation Module (New England Biolabs) and fragmented by heating at 94°C for 15 min. The fragmented RNA was reverse transcribed with random primers. After second-strand DNA synthesis, the cDNA fragments were dA tailed and adaptor ligated. PCR amplification was carried out to get sufficient amount of libraries for sequencing. The libraries were sequenced on an Illumina Hiseq2500 in single-end mode (Illumina). Sequencing reads were mapped to human genome hg19 using Tophat 2.0.13 (Trapnell et al., 2009). The expression level of each gene was quantified with normalized FPKM (fragments per kilobase of exon per million mapped fragments) using Cufflinks 2.2.1 (Trapnell et al., 2010). Gene set enrichment analysis was carried out using GSEA v2.2.2 (Broad Institute) with expression data downloaded from GEO: GSE6008 (Hendrix et al., 2006) and the set of upregulated genes in double-mutant cells as gene set input. The default enrichment cutoff was used in the analysis.

Dnase-I Hypersensitive Site Sequencing

DNase-seq libraries were prepared from ~1 million cells following a published protocol with minor modifications (He et al., 2014). The nuclei were digested with DNase I (Roche) at 60 U/mL final concentration at 37°C for 5 min. The reactions were stopped by adding stop buffer containing EDTA and proteinase K. DNA was purified by phenyl-chloroform extraction and ethanol precipitation. Small fragments around 150 bp were selected with SPRIselect (Beckman Coulter). Sequencing libraries were prepared with NEBNext Ultra DNA Library Prep Kit for Illumina (New England Biolabs). The libraries were sequenced on an Illumina Hiseq2500 in single-end mode (Illumina). Sequencing reads were mapped to human genome hg19 using Bowtie2 2.1.0 (Langmead and Salzberg, 2012). Differential DHSs with 3-fold difference were called using ChIPDiff (Xu et al., 2008).

---

indicated treatment, and tumor sizes were measured on the indicated days (n = 5 per group). Statistical analysis comparing combined treatment and single treatments is performed (either carboplatin only or IKK-IIV only, which resulted in the same range of p values). Error bars indicate SEM.

(D) Image of dissected tumors at the time of mouse sacrifice shown in (C). Scale bar, 5 cm.

(E) Working model of how ARID1A/PIK3CA mutation induces cytokine expression. (a) In wild-type cells, cytokine genes are repressed by the Sin3A-HDAC complex recruited by ARID1A. At the same time, RelA is sequestered by IκB. (b) In ARID1A mutant cells, the recruitment of the Sin3-HDAC complex is abolished, leading to histone acetylation. However, RelA is still sequestered by IκB. Thus, cytokine induction is limited. (c) In PIK3CA active cells, the AKT-IKK2 pathway releases RelA from IκB. However, the presence of the Sin3A-HDAC complex limits cytokine induction. (d) In the presence of both mutations, cytokine genes are robustly induced, which contributes to cell proliferation and drug resistance.

**p < 0.01; ***p < 0.001. See also Figure S7.

Statistical Analysis

All graphs were drawn using GraphPad Prism. Statistical analyses were performed by paired Student's t test (two tailed) comparing indicated pairs in each figure.

SUPPLEMENTAL INFORMATION

Supplemental Information includes seven figures and two tables and can be found with this article online at http://dx.doi.org/10.1016/j.celrep.2016.09.003.

ACCESSION NUMBERS

The accession number for the sequencing data generated in this study is GEO: GSE86004.

AUTHOR CONTRIBUTIONS

M.K. and Y.Z. conceived the project, interpreted the data, and wrote the manuscript; M.K performed most of the experiments; and F.L. performed RNA-seq and DNase-seq analyses.

REFERENCES

Acharyya, S., Oskarsson, T., Vanharanta, S., Malladi, S., Kim, J., Morris, P.G., Manova-Todorova, K., Leversha, M., Hogg, N., Seshan, V.E., et al. (2012). A CXCL1 paracrine network links cancer chemoresistance and metastasis. Cell *150*, 165–178.

Bast, R.C., Jr., Hennessy, B., and Mills, G.B. (2009). The biology of ovarian cancer: new opportunities for translation. Nat. Rev. Cancer *9*, 415–428.

Baud, V., and Karin, M. (2009). Is NF-kappaB a good target for cancer therapy? Hopes and pitfalls. Nat. Rev. Drug Discov. *8*, 33–40.

Bitler, B.G., Aird, K.M., Garipov, A., Li, H., Amatangelo, M., Kossenkov, A.V., Schultz, D.C., Liu, Q., Shih, IeM., Conejo-Garcia, J.R., et al. (2015). Synthetic lethality by targeting EZH2 methyltransferase activity in ARID1A-mutated cancers. Nat. Med. *21*, 231–238.

Brown, K., Gerstberger, S., Carlson, L., Franzoso, G., and Siebenlist, U. (1995). Control of I kappa B-alpha proteolysis by site-specific, signal-induced phosphorylation. Science *267*, 1485–1488.

Chandler, R.L., Damrauer, J.S., Raab, J.R., Schisler, J.C., Wilkerson, M.D., Didion, J.P., Starmer, J., Serber, D., Yee, D., Xiong, J., et al. (2015). Coexistent ARID1A-PIK3CA mutations promote ovarian clear-cell tumorigenesis through pro-tumorigenic inflammatory cytokine signalling. Nat. Commun. *6*, 6118.

Gerritsen, M.E., Williams, A.J., Neish, A.S., Moore, S., Shi, Y., and Collins, T. (1997). CREB-binding protein/p300 are transcriptional coactivators of p65. Proc. Natl. Acad. Sci. USA *94*, 2927–2932.

Grivennikov, S.I., and Karin, M. (2010). Dangerous liaisons: STAT3 and NF-kappaB collaboration and crosstalk in cancer. Cytokine Growth Factor Rev. *21*, 11–19.

Grivennikov, S., Karin, E., Terzic, J., Mucida, D., Yu, G.Y., Vallabhapurapu, S., Scheller, J., Rose-John, S., Cheroutre, H., Eckmann, L., and Karin, M. (2009). IL-6 and Stat3 are required for survival of intestinal epithelial cells and development of colitis-associated cancer. Cancer Cell *15*, 103–113.

Harikrishnan, K.N., Chow, M.Z., Baker, E.K., Pal, S., Bassal, S., Brasacchio, D., Wang, L., Craig, J.M., Jones, P.L., Sif, S., and El-Osta, A. (2005). Brahma links the SWI/SNF chromatin-remodeling complex with MeCP2-dependent transcriptional silencing. Nat. Genet. *37*, 254–264.

He, H.H., Meyer, C.A., Hu, S.S., Chen, M.W., Zang, C., Liu, Y., Rao, P.K., Fei, T., Xu, H., Long, H., et al. (2014). Refined DNase-seq protocol and data analysis reveals intrinsic bias in transcription factor footprint identification. Nat. Methods *11*, 73–78.

Hendrix, N.D., Wu, R., Kuick, R., Schwartz, D.R., Fearon, E.R., and Cho, K.R. (2006). Fibroblast growth factor 9 has oncogenic activity and is a downstream target of Wnt signaling in ovarian endometrioid adenocarcinomas. Cancer Res. *66*, 1354–1362.

Horie, R. (2013). Molecularly-targeted Strategy and NF-κB in lymphoid malignancies. J. Clin. Exp. Hematop. *53*, 185–195.

Iliopoulos, D., Hirsch, H.A., and Struhl, K. (2009). An epigenetic switch involving NF-kappaB, Lin28, Let-7 MicroRNA, and IL6 links inflammation to cell transformation. Cell *139*, 693–706.

Jones, S., Wang, T.L., Shih, IeM., Mao, T.L., Nakayama, K., Roden, R., Glas, R., Slamon, D., Diaz, L.A., Jr., Vogelstein, B., et al. (2010). Frequent mutations of chromatin remodeling gene ARID1A in ovarian clear cell carcinoma. Science *330*, 228–231.

Kadoch, C., and Crabtree, G.R. (2015). Mammalian SWI/SNF chromatin remodeling complexes and cancer: Mechanistic insights gained from human genomics. Sci. Adv. *1*, e1500447.

Kane, L.P., Shapiro, V.S., Stokoe, D., and Weiss, A. (1999). Induction of NF-kappaB by the Akt/PKB kinase. Curr. Biol. *9*, 601–604.

Karin, M., Yamamoto, Y., and Wang, Q.M. (2004). The IKK NF-kappa B system: a treasure trove for drug development. Nat. Rev. Drug Discov. *3*, 17–26.

Kim, J.W., Jang, S.M., Kim, C.H., An, J.H., Kang, E.J., and Choi, K.H. (2012). New molecular bridge between RelA/p65 and NF-κB target genes via histone acetyltransferase TIP60 cofactor. J. Biol. Chem. *287*, 7780–7791.

Kumar, J., and Ward, A.C. (2014). Role of the interleukin 6 receptor family in epithelial ovarian cancer and its clinical implications. Biochim. Biophys. Acta *1845*, 117–125.

Lai, A.Y., and Wade, P.A. (2011). Cancer biology and NuRD: a multifaceted chromatin remodelling complex. Nat. Rev. Cancer *11*, 588–596.

Langmead, B., and Salzberg, S.L. (2012). Fast gapped-read alignment with Bowtie 2. Nat. Methods *9*, 357–359.

Liu, J., Yang, G., Thompson-Lanza, J.A., Glassman, A., Hayes, K., Patterson, A., Marquez, R.T., Auersperg, N., Yu, Y., Hahn, W.C., et al. (2004). A genetically defined model for human ovarian cancer. Cancer Res. *64*, 1655–1663.

Mackay, H.J., Hirte, H., Colgan, T., Covens, A., MacAlpine, K., Grenci, P., Wang, L., Mason, J., Pham, P.A., Tsao, M.S., et al. (2010). Phase II trial of the histone deacetylase inhibitor belinostat in women with platinum resistant epithelial ovarian cancer and micropapillary (LMP) ovarian tumours. Eur. J. Cancer *46*, 1573–1579.

Mercurio, F., Zhu, H., Murray, B.W., Shevchenko, A., Bennett, B.L., Li, J., Young, D.B., Barbosa, M., Mann, M., Manning, A., and Rao, A. (1997). IKK-1 and IKK-2: cytokine-activated IkappaB kinases essential for NF-kappaB activation. Science *278*, 860–866.

Minucci, S., and Pelicci, P.G. (2006). Histone deacetylase inhibitors and the promise of epigenetic (and more) treatments for cancer. Nat. Rev. Cancer *6*, 38–51.

Nakanishi, C., and Toi, M. (2005). Nuclear factor-kappaB inhibitors as sensitizers to anticancer drugs. Nat. Rev. Cancer *5*, 297–309.

Napetschnig, J., and Wu, H. (2013). Molecular basis of NF-κB signaling. Annu. Rev. Biophys. *42*, 443–468.

Neph, S., Vierstra, J., Stergachis, A.B., Reynolds, A.P., Haugen, E., Vernot, B., Thurman, R.E., John, S., Sandstrom, R., Johnson, A.K., et al. (2012). An expansive human regulatory lexicon encoded in transcription factor footprints. Nature *489*, 83–90.

Perkins, N.D., Felzien, L.K., Betts, J.C., Leung, K., Beach, D.H., and Nabel, G.J. (1997). Regulation of NF-kappaB by cyclin-dependent kinases associated with the p300 coactivator. Science *275*, 523–527.

Romashkova, J.A., and Makarov, S.S. (1999). NF-kappaB is a target of AKT in anti-apoptotic PDGF signalling. Nature *401*, 86–90.

Samartzis, E.P., Noske, A., Dedes, K.J., Fink, D., and Imesch, P. (2013). ARID1A mutations and PI3K/AKT pathway alterations in endometriosis and endometriosis-associated ovarian carcinomas. Int. J. Mol. Sci. *14*, 18824–18849.

Samuels, Y., Diaz, L.A., Jr., Schmidt-Kittler, O., Cummins, J.M., Delong, L., Cheong, I., Rago, C., Huso, D.L., Lengauer, C., Kinzler, K.W., et al. (2005). Mutant PIK3CA promotes cell growth and invasion of human cancer cells. Cancer Cell *7*, 561–573.

Schafer, Z.T., and Brugge, J.S. (2007). IL-6 involvement in epithelial cancers. J. Clin. Invest. *117*, 3660–3663.

Schwitalla, S., Fingerle, A.A., Cammareri, P., Nebelsiek, T., Göktuna, S.I., Ziegler, P.K., Canli, O., Heijmans, J., Huels, D.J., Moreaux, G., et al. (2013). Intestinal tumorigenesis initiated by dedifferentiation and acquisition of stem-cell-like properties. Cell *152*, 25–38.

Sun, S.C. (2011). Non-canonical NF-κB signaling pathway. Cell Res. *21*, 71–85.

Suryo Rahmanto, Y., Jung, J.G., Wu, R.C., Kobayashi, Y., Heaphy, C.M., Meeker, A.K., Wang, T.L., and Shih, I.M. (2016). Inactivating ARID1A tumor suppressor enhances TERT transcription and maintains telomere length in cancer cells. J. Biol. Chem *291*, 9690–9699.

Takahashi, H., Ogata, H., Nishigaki, R., Broide, D.H., and Karin, M. (2010). Tobacco smoke promotes lung tumorigenesis by triggering IKKbeta- and JNK1-dependent inflammation. Cancer Cell *17*, 89–97.

Trapnell, C., Pachter, L., and Salzberg, S.L. (2009). TopHat: discovering splice junctions with RNA-Seq. Bioinformatics *25*, 1105–1111.

Trapnell, C., Williams, B.A., Pertea, G., Mortazavi, A., Kwan, G., van Baren, M.J., Salzberg, S.L., Wold, B.J., and Pachter, L. (2010). Transcript assembly and quantification by RNA-Seq reveals unannotated transcripts and isoform switching during cell differentiation. Nat. Biotechnol. *28*, 511–515.

Wang, Y., Zhang, H., Chen, Y., Sun, Y., Yang, F., Yu, W., Liang, J., Sun, L., Yang, X., Shi, L., et al. (2009). LSD1 is a subunit of the NuRD complex and targets the metastasis programs in breast cancer. Cell *138*, 660–672.

Waugh, D.J., and Wilson, C. (2008). The interleukin-8 pathway in cancer. Clin. Cancer Res. *14*, 6735–6741.

Wiegand, K.C., Shah, S.P., Al-Agha, O.M., Zhao, Y., Tse, K., Zeng, T., Senz, J., McConechy, M.K., Anglesio, M.S., Kalloger, S.E., et al. (2010). ARID1A mutations in endometriosis-associated ovarian carcinomas. N. Engl. J. Med. *363*, 1532–1543.

Wilson, B.G., and Roberts, C.W. (2011). SWI/SNF nucleosome remodellers and cancer. Nat. Rev. Cancer *11*, 481–492.

Xia, Y., Shen, S., and Verma, I.M. (2014). NF-κB, an active player in human cancers. Cancer Immunol. Res. *2*, 823–830.

Xu, H., Wei, C.L., Lin, F., and Sung, W.K. (2008). An HMM approach to genome-wide identification of differential histone modification sites from ChIP-seq data. Bioinformatics *24*, 2344–2349.

Yamaguchi, K., Mandai, M., Oura, T., Matsumura, N., Hamanishi, J., Baba, T., Matsui, S., Murphy, S.K., and Konishi, I. (2010). Identification of an ovarian clear cell carcinoma gene signature that reflects inherent disease biology and the carcinogenic processes. Oncogene *29*, 1741–1752.

Yamamoto, S., Tsuda, H., Takano, M., Tamai, S., and Matsubara, O. (2012). Loss of ARID1A protein expression occurs as an early event in ovarian clear-cell carcinoma development and frequently coexists with PIK3CA mutations. Mod. Pathol. *25*, 615–624.

Zang, Z.J., Cutcutache, I., Poon, S.L., Zhang, S.L., McPherson, J.R., Tao, J., Rajasegaran, V., Heng, H.L., Deng, N., Gan, A., et al. (2012). Exome sequencing of gastric adenocarcinoma identifies recurrent somatic mutations in cell adhesion and chromatin remodeling genes. Nat. Genet. *44*, 570–574.

Zhang, Y., Iratni, R., Erdjument-Bromage, H., Tempst, P., and Reinberg, D. (1997). Histone deacetylases and SAP18, a novel polypeptide, are components of a human Sin3 complex. Cell *89*, 357–364.

Zhang, Y., LeRoy, G., Seelig, H.P., Lane, W.S., and Reinberg, D. (1998). The dermatomyositis-specific autoantigen Mi2 is a component of a complex containing histone deacetylase and nucleosome remodeling activities. Cell *95*, 279–289.

Zhang, H.S., Gavin, M., Dahiya, A., Postigo, A.A., Ma, D., Luo, R.X., Harbour, J.W., and Dean, D.C. (2000). Exit from G1 and S phase of the cell cycle is regulated by repressor complexes containing HDAC-Rb-hSWI/SNF and Rb-hSWI/SNF. Cell *101*, 79–89.